Scattering from rough inhomogeneous media: splitting of surface and volume scattering

A. Sentenac, H. Giovannini, and M. Saillard

Institut Fresnel, Université de St Jérôme, 13 397 Marseille Cedex 20, France

Received March 9, 2001; revised manuscript received July 11, 2001; accepted September 4, 2001

The intensity scattered by particles randomly placed beneath a rough interface is studied with rigorous simulations. It is shown that the angular intensity pattern is close to that obtained by adding the intensity scattered by particles under a flat surface to that scattered by a rough homogeneous surface whose permittivity is evaluated with an effective-medium theory. This heuristic splitting rule is accurate for a large range of parameters that are well beyond any perturbative treatment. © 2002 Optical Society of America

OCIS codes: 290.5850, 290.5880, 290.3030.

1. INTRODUCTION

We consider the scattering of electromagnetic waves from a semi-infinite homogeneous medium (or binder) with a rough interface that contains many randomly placed scatterers (see Fig. 1 below). The study of scattering from rough inhomogeneous media involving both surface and volume effects finds applications in different domains: from the microwave domain,[1,2] with the remote sensing from natural media in particular, to the optical domain, where the properties of composite materials such as polymers or paints with metallic inclusions are of interest (for designing light absorbers, for instance).

Many approximate models, empirical or analytical, have been proposed to analyze the scattering from this kind of geometry, especially in the radar and microwave communities. A commonly used heuristic approach assumes that the electromagnetic fields are spatially incoherent in the inhomogeneous bulk. The specific intensity inside the medium is calculated with the phenomenological transfer radiative equation.[1,2] The volume scattering process is then described by the phase matrix, which is often evaluated under the single-scattering approximation by the scattering matrix of one scatterer. The rough interface intervenes as a top boundary condition on the specific intensity through the surface-scattering transmission and the reflection phase matrix. The latter is built from the bidirectional reflection and transmission coefficients of the rough surface of the binding medium.[3] The scattering from a homogeneous rough surface can be obtained with various approximate models such as the Kirchhoff approximation, the integral equation method, perturbative techniques or other methods.[3] Some approaches use solely the electromagnetism formalism. A perturbative development of the field with respect to the root mean square height of the surface and/or to the dielectric contrast of the inhomogeneities[4–6] is usually proposed to solve the Maxwell equations. In some models, such as the Born approximation or the distorted-wave Born approximation,[7,8] roughness and volume inhomogeneities are accounted for in the same way in a volume integral equation. Both are considered permittivity fluctuations of a reference medium (vacuum in the classic Born approximation, semi-infinite homogeneous medium in the distorted-wave Born approximation). Then a perturbative solution of the integral equation with respect to the dielectric contrast is derived. Widely used in the x-ray community in its simplest form, this approach has recently been applied, through the introduction of a more complicated reference medium (a semi-infinite medium with graded index),[9] to higher dielectric contrasts such as those encountered in the optical and radar domains. The validity domain of the mean-field theory with respect to the rms height, correlation length, and scatterer size proves to be larger than in many other approximate techniques as long as the permittivity contrast remains smaller than 3.[9,10]

On the other hand, few rigorous numerical methods have been developed, to our knowledge, to simulate the scattering from rough inhomogeneous media, even when the system presents one axis of invariance. We quote the boundary integral method[11,12] for the two-dimensional and three-dimensional problem with only one scatterer. For the two-dimensional geometry, with many scatterers in the binder, we find finite-element methods,[13,14] a combined surface and volume integral,[15] and the differential method as well as a combination of the S matrix and of the integral formalisms.[16] Owing to the large number of unknowns, the rigorous numerical simulation of scattering from rough inhomogeneous media remains a difficult task, and there is a need for empirical rules that could permit one to simplify the scattering issue.

In the perturbative theory presented in Ref. 4, it is shown that scattering from rough inhomogeneous media can be split into two contributions, one stemming from the surface of the binder and the other from the volume. These contributions can be added incoherently to represent the scattering from rough inhomogeneous media. This approach was tested in Ref. 13, but a difference was found with the rigorous simulations of the scattering problem. In the more elaborate perturbative expansion of the mean-field theory,[17] a similar splitting into two independent contributions is also found. Yet in this case the permittivity of the homogeneous surface is not that of the binder (see Fig. 2 below). It depends on the permit-

0740-3232/2002/040727-10$15.00

tivity of the binding medium and on the size, density, and permittivity of the inhomogeneities. A better agreement is then found between the incoherent superposition of the scattering and the rigorous results.[17]

Our aim in this paper is to determine whether it is possible to evaluate the scattering pattern from rough inhomogeneous media by studying two independent and simpler problems involving solely surface or solely volume scattering processes for cases that are outside the domain of validity of approximate methods. A wide range of parameters such as the rms height of the surface, density of the particles, and contrast of the permittivity are investigated to illustrate the relevance of the splitting. The behaviors of both the off-specular diffuse pattern and the specular beam are analyzed.

In Section 2 we describe the theoretical and numerical methods used to compute scattering from rough inhomogeneous media. Various techniques for determining the value of the effective permittivity are also described. We point out the importance of determining its value accurately.

In Section 3 we present numerical experiments that show that the splitting rule works for geometries that are well beyond the domain of validity of perturbation theories. The shift of the Brewster angle, due to roughness and volume scattering, is also retrieved with accuracy.

Finally, Section 4 is devoted to a more complicated problem. By depositing an optimized coating on a rough inhomogeneous medium, we are able to reduce the surface-scattering contribution and thus to enhance the volume-scattering visibility.

2. THEORETICAL AND NUMERICAL TOOLS

In this section we first present the numerical techniques that enable us to do rigorous simulations of scattering from rough inhomogeneous films. Since they have already been presented in Ref. 16, we only point out their basic principles; readers are referred to Ref. 16 for more detailed explanations. In Subsection 2.C we focus on the evaluation of the effective permittivity, which is the key point in the splitting between surface and volume scattering.

A. Description of the Problem and Notation

The structure under study consists of a set of parallel homogeneous rods, embedded in a semi-infinite homogeneous medium (binder), separated from the upper medium (air) by a one-dimensional rough interface. The geometry, schematically represented in Fig. 1, is invariant along the y axis, and the surface profile C_1 is described by a differentiable function $z = s(x)$. The complex permittivity is equal to ϵ_0 if $z > s(x)$, ϵ_{sc} inside the rods, and ϵ_b in the binder. The permeability is assumed to be that of vacuum everywhere.

The incident field is represented either by an s- or p-polarized monochromatic Gaussian beam with pulsation ω, and an $\exp(-i\omega t)$ time dependence is assumed for the complex amplitudes. Denoting by F^{inc} either the electric or the magnetic incident field depending on whether the polarization is s or p, we have

$$F^{inc}(x, z) = \int_{-\infty}^{+\infty} p(\alpha - \alpha_0)\exp[i\alpha x - i\gamma(\alpha)z]\mathrm{d}\alpha, \tag{1}$$

where

$$p(\alpha) = w \exp(-w^2\alpha^2/2), \tag{2}$$

$$\alpha_0 = k_0 \sin\theta^{inc} \tag{3}$$

$$\gamma = (k_0^2 - \alpha^2)^{1/2}, \qquad \mathrm{Im}(\gamma) \geqslant 0. \tag{4}$$

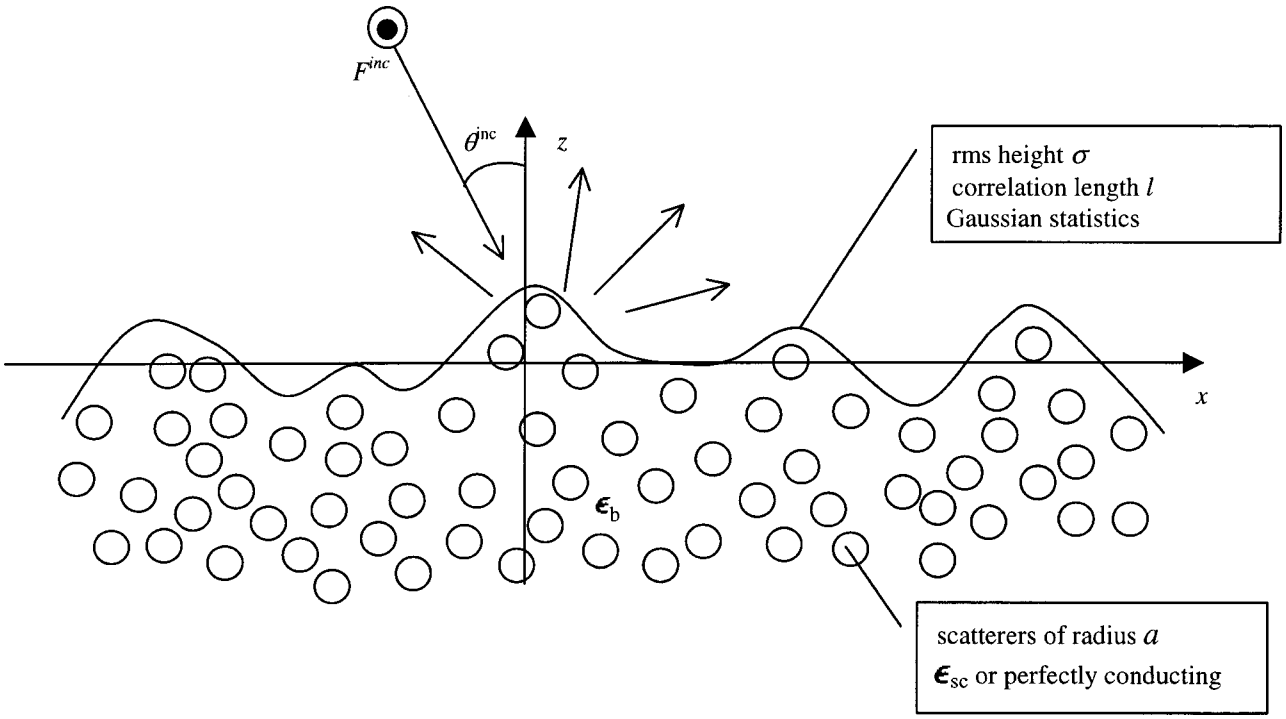

Fig. 1. Geometry and notation.

The parameters w (beam waist) and θ^{inc} (mean angle of incidence) characterize the incident beam, and k_0 represents the wave number in the upper medium. The total and the diffracted fields are denoted by F and $F^d = F - F^{\text{inc}}$, respectively, and above the highest excursion of the surface profile the diffracted field can be written as a superposition of outgoing plane waves:

$$F^d(x, z) = \int B(\alpha)\exp[i\alpha x + i\gamma(\alpha)z]\mathrm{d}\alpha. \quad (5)$$

The differential reflection coefficient, which gives the part of the incident energy scattered into an angular interval $\delta\theta_s$ about the scattering direction defined by the scattering angle θ_s, is written as

$$\frac{\partial R}{\partial \theta_s} = \frac{|\gamma(\alpha_s)B(\alpha_s)|^2}{P^{\text{inc}}}, \quad (6)$$

where $\alpha_s = k_0 \sin\theta_s$ and P^{inc} is the total incident flux through a horizontal plane:

$$P^{\text{inc}} = \int \gamma(\alpha)|p(\alpha - \alpha_0)|^2\mathrm{d}\alpha. \quad (7)$$

B. Solution of the Scattering Problem

Two methods have been used to solve the scattering problems. The differential method, on the one hand, is very general: It can deal with inhomogeneous media and also more complicated geometries such as inhomogeneous media covered by a coating, but it remains numerically costly. On the other hand, we have developed a boundary integral method that is less general but speeded up thanks to a hybrid representation of the scattered field.

In the differential method, the inhomogeneous medium is described by the complex wave number $k(x, z)$ whose variations are restricted to a layer of thickness D. The fact that those fluctuations may stem from the presence of rough surfaces or buried objects has no effect on the numerical scheme. Above and below the perturbed region, the field is written as a Rayleigh expansion such as Eq. (5). Inside the perturbed region, Maxwell equations yield a first-order differential system for $(E_y, \partial E_y/\partial z)$ in s polarization and $(\partial H_y/\partial z, \partial H_y/k^2\partial z)$ in p polarization that can be solved in the Fourier space, for instance by a Runge–Kutta algorithm. In s polarization, denoting by $e(\alpha, z)$ and $\Delta\kappa(\alpha, z)$ the Fourier transform of $E_y(x, z)$ and $k^2(x, z)$, respectively, Maxwell equations yield

$$\frac{\partial^2 e(\alpha, z)}{\partial z^2} + \int \Delta\kappa(\alpha - \alpha', z)e(\alpha', z)\mathrm{d}\alpha' = 0, \quad (8)$$

which can be written in matrix notation as

$$\frac{\mathrm{d}}{\mathrm{d}z}\begin{bmatrix}\mathbf{e}\\ \dfrac{\partial \mathbf{e}}{\partial z}\end{bmatrix}(z) = \mathbf{T}(z)\begin{bmatrix}\mathbf{e}\\ \dfrac{\partial \mathbf{e}}{\partial z}\end{bmatrix}(z), \quad (9)$$

where $\mathbf{e}_i(z) = e(i\Delta\alpha, z)$ and $\Delta\alpha$ is the sampling step in the Fourier space. The differential system and the continuity of E_y and $\partial E_y/\partial z$ at $z = 0$ and $z = D$ allow us to evaluate the scattered amplitudes $B(\alpha)$ and the differential reflection coefficient using Eq. (6). A slightly more complicated differential system is written for p polarization. The numerical implementation of this formalism is straightforward but requires a careful testing of the convergence with respect to the various samplings and truncations. The S-matrix algorithm[18] and astute truncating of the Fourier coefficients[19] have drastically improved the convergence rate and the significance of this technique. The results given by the differential method are in agreement with that of the surface integral method.[16]

In the second approach, the field scattered by the rough surface is classically derived from a surface density, but that from the rods is expanded as a Fourier–Bessel series. In the case of scatterers with dimensions smaller than the wavelength, only a few terms of this expansion are required, leading to a drastic reduction of the number of unknowns, as compared with a classical integral method. Above the surface, the scattered field is thus written as a single-layer potential with density ϕ_1, leading to

$$F(P) = F^{\text{inc}} + \int_{C_1} G(P, M')\phi_1(M')\mathrm{d}s', \quad (10)$$

where $G(P, M') = -i/4H_0^{(1)}(k_0PM')$ denotes the free-space Green's function. Denoting by F_j^R the Fourier–Bessel expansion of the field scattered by the jth rod in terms of outgoing Hankel functions, we get

$$F_j^R(P) = \sum_{n=-\infty}^{+\infty} b_n^{(j)}H_n^{(1)}(k_b r_j)\exp(in\theta_j), \quad (11)$$

where k_b represents the wave number of the surrounding medium, i.e., of the binder, and where r_j and θ_j are the local polar coordinates, associated with the jth scatterer, of P. Hence the field in the semi-infinite medium below the surface is written as the sum of the boundary integral and Fourier series

$$F(P) = \int_{C_1} K(P, M')\phi_1(M')\mathrm{d}s' + \sum_{j>1} F_j^R(P), \quad (12)$$

where the kernel K contains the Green's function in both media, as well as their normal derivatives. This equation is rigorous as long as one can plot nonintersecting circles surrounding each scatterer that do not intersect C_1. The unknown surface density ϕ_1 and the unknown scattering amplitudes $b_n^{(j)}$ are linked through the boundary conditions on the surface and through the scattering matrices of the buried scatterers. The scattering matrix for each scatterer must be either known analytically or computed by other means. This is the price for fast solution.

The validity of this approach has been tested by comparing the approach with the standard integral method. For circular rods with radius a such that $k_0a < 0.5$, one gets better than a few percent accuracy with three terms from the Bessel expansion. Typically, the number of unknowns is thus reduced by a factor of 5. This permits one to solve scattering problems with a large number of small scatterers at low computational cost. Combined with the beam simulation method, this permits one to deal with samples of arbitrary size and almost any density of scatterers, provided that either the penetration depth or the thickness of the inhomogeneous layer remains finite. Let us point out that the penetration depth is governed both

by absorption and by diffusion, each contributing to the imaginary part of the effective permittivity, which now has to be estimated to define the equivalent surface-scattering problem.

C. Estimation of the Effective Permittivity

The main point of this paper is to show that the scattering from a rough medium filled with many scatterers can be separated into surface and volume contributions for a large range of parameters (like the rms height or the density of the scatterers). In the following, we restrict our study to cylindrical rods that are all identical, with a circular cross section of radius a, and to surface roughnesses that follow Gaussian statistics with rms height σ and Gaussian correlation function with correlation length l.

The splitting process has already been investigated by Pak *et al.*[13] To simulate the scattering from an inhomogeneous rough medium, they have added incoherently the scattered intensity of the particles, placed in the binder under a flat interface, to that of the rough binder alone. Yet the agreement with the rigorous results was not satisfactory in some cases. To improve the splitting process, we propose to modify the surface contribution by considering a rough homogeneous medium whose permittivity accounts for the presence of the particles in the binder. The effective dielectric constant will then express the coupling between surface and volume scattering. In Fig. 2(a) we plot the scattered intensity of a rough inhomogeneous medium made of a binder of permittivity $\epsilon_b = 2$, where scatterers of radius $a = 0.035\lambda$ and permittivity $\epsilon_{sc} = 9 + i3.5$ with volume density $d = 0.2$ have been randomly placed. The random medium is illuminated under normal incidence by a Gaussian beam with waist $w = 5\lambda$. The roughness parameters are chosen such that the surface and volume contributions appear naturally in the angular behavior of the scattering pattern. The correlation length being $l = \lambda$ and the rms height being $\sigma = \lambda/10$, the surface-scattering contribution is important close to the specularly reflected beam. In contrast, volume scattering is almost constant whatever the scattering angles; hence it is clearly visible at high angles when the surface scattering becomes negligible. This interpretation is confirmed by the dotted and the dash-dot-dot curves of Fig. 2(a), which respectively represent the scattered intensity of the particles in the binder under a flat surface (volume contribution) and the scattered intensity of an homogeneous rough surface with the same statistical characteristics as the inhomogeneous medium but with a carefully evaluated effective permittivity. In Fig. 2(b) we compare the scattering pattern of the inhomogeneous medium with the sums of the volume-scattering intensities with either the effective rough surface contribution or the binder rough surface contribution. It is clear that taking an effective permittivity for the surface contribution gives much better results. The superposition of the effective surface-scattered intensity with the incoherent scattering of the particles under a flat surface permits us to represent accurately the incoherent scattering and the coherent peak of the inhomogeneous rough medium.

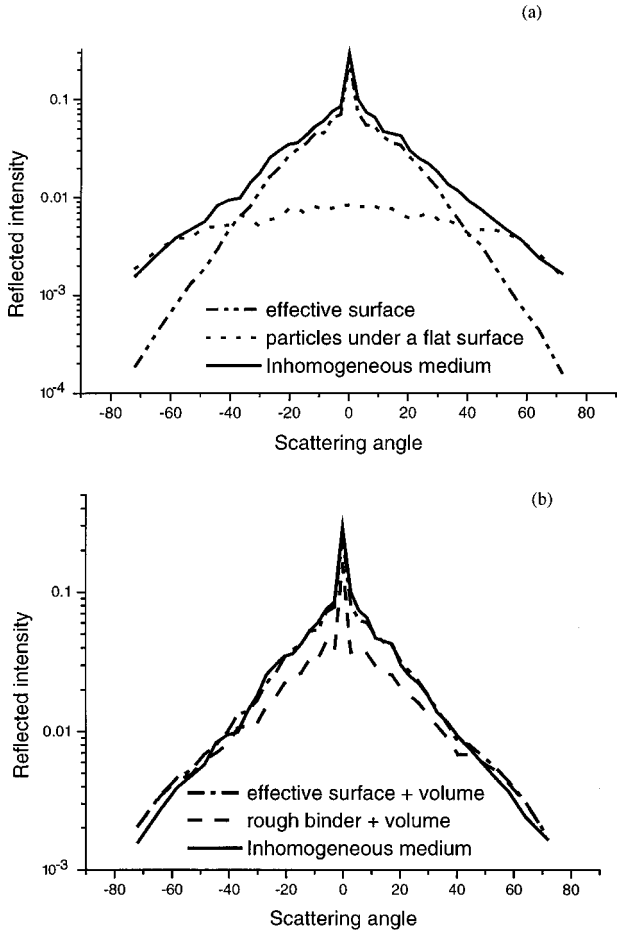

Fig. 2. Scattered intensity of various geometries illuminated under normal incidence; s polarization, $w = 5\lambda$. Binder, $\epsilon_b = 2$, $\sigma = 0.1\lambda$, $l = \lambda$; scatterers, $d = 0.2$, $a = 0.035\lambda$, $\epsilon_{sc} = 9 + i3.5$. Solid curve, rough inhomogeneous medium; dash-dot-dot curve, rough effective surface. Same roughness parameters as the inhomogeneous medium. Dotted curve, particles under a flat surface; same parameters as that of the inhomogeneous medium, but the binder is flat. The effective permittivity is numerically evaluated, $\epsilon_{eff} = 2.35 + i0.65$.

The introduction of an effective permittivity comes from an analysis of the expression of the scattered intensity from rough inhomogeneous media obtained with the mean-field theory.[17] In the simple case of one-dimensional inhomogeneous surfaces illuminated by an s-polarized wave, the model shows that the scattered intensity can be separated into surface- and a volume-scattering contributions. The volume-scattering contribution is close to that given by particles embedded in the binder under a flat interface, when solely the incoherent part is considered. The surface-scattering term comes from a rough surface whose effective dielectric constant ϵ_{eff} is the average of the permittivity of the binder and that of the scatterers with respect to their surface density,

$$\epsilon_{eff} = \epsilon_b(1 - d) + d\,\epsilon_{sc}. \tag{13}$$

This result is obtained *without any heuristic hypothesis*, by working out a perturbative treatment (or Born series) of an exact volume integral equation involving the electric field and the Green's function of a carefully chosen reference medium. Extension to the p-polarized case is more difficult and necessitates a phenomenological approach. The effective permittivity is then given by Bruggeman formulas written for a two-dimensional problem:

$$\epsilon_{\mathrm{eff}}^2 + (1 - 2d)(\epsilon_{\mathrm{sc}} - \epsilon_b)\epsilon_{\mathrm{eff}} - \epsilon_{\mathrm{sc}}\epsilon_b = 0. \quad (14)$$

These effective permittivities permit us to describe correctly the behavior of the mean (or coherent) field in a slab of randomly placed scatterers under several restrictions inherent to the Born approximation, which underlies the mean-field theory. The dielectric contrast and the size of the scatterers should satisfy the conditions of the Rayleigh–Gans approximation[20]:

$$|\epsilon_{\mathrm{sc}} - \epsilon_b| \ll 1, \quad (15a)$$

$$2\pi 2a|\epsilon_{\mathrm{sc}} - \epsilon_b|/\lambda \ll 1. \quad (15b)$$

Note that the effective permittivities given by Eqs. (13) and (14) remain real when both ϵ_{sc} and ϵ_b are real, so the attenuation of the mean field due to diffusion is not accounted for. Hence the slab should be thin enough that the diffusion-induced losses are negligible. This could also be achieved if absorption losses were greater than diffusion losses.

To improve the determination of the effective permittivity for problems where these various restrictions do not hold, for example when the scatterers are metallic, we have considered the results of effective-medium theory. It can be shown that, under several hypotheses, the mean field in a random medium behaves as if it were propagating in a homogeneous medium with an effective complex permittivity.[1,21] Several expressions of the effective dielectric constant have been proposed depending on the degree of their approximations. For instance, the Foldy approximation and the quasi-crystalline approximation give expressions of an effective dielectric constant that account for the attenuation of the mean field caused by single-scattering and double-scattering processes, respectively. We have chosen a simple formulation proposed in Ref. 22 whose confrontation with experimental data was satisfactory.[23] This formula is derived from a perturbative solution of the Dyson equation for the mean field. It necessitates the scattering matrix of the particles and the pair-correlation function g of their centers. The wave scattered by a cylindrical object can be written in the far field of the surrounding homogeneous medium with wave number k_b as

$$E_d(r, \theta) \approx \sqrt{\frac{2}{\pi k_b r}} \exp(ik_b r - i\pi/4) f(\theta). \quad (16)$$

In s polarization and for small enough cylinders, the scattering amplitude f is constant. For perfect conductors, it may be approximated with good accuracy by $f = -J_0(k_b a)/H_0(k_b a)$ for $a < 0.05\ \lambda$. The pair-correlation function is obtained from the probability density of scatterer 1 being at $\mathbf{x}_1$ and scatterer 2 being at $\mathbf{x}_2$, $P(\mathbf{x}_1, \mathbf{x}_2)$. Assuming that P depends solely on $r = |\mathbf{x}_1 - \mathbf{x}_2|$, one gets $g(r) = S^2 P(r) - 1$, where S is the area of the domain in which the cylinders have been placed. For densities smaller than 5%, g is approximated by a step function equal to -1 for $r < 4a$ and 0 for $r > 4a$. For denser media, $g(r)$ is evaluated with Monte Carlo simulations in which the scatterers are randomly distributed with the constraint that they cannot interpenetrate each other. The effective dielectric constant is then calculated through

$$K^2 = k_b{}^2 + 4i\rho f - (4\rho f)^2 k_b{}^{-1} \int_0^\infty \exp(ik_b r) g(r) \sin g(k_b r) \mathrm{d}r, \quad (17)$$

where ρ is the number density equal to $d/(\pi a^2)$. When the scattering amplitude is not constant, in p polarization for instance, we replace f in Eq. (17) with the forward-scattering amplitude, i.e., $f(\pi)$ if the angle of the incident plane wave is $\theta = 0$ as proposed in Ref. 23. When the scatterers satisfy conditions (15) and (16), we verify that the real part of the effective permittivity obtained with Eq. (17) is close to that given by Eq. (13) in s polarization and Eq. (14) in p polarization. Yet Eq. (17) also provides an imaginary part, depending on the volume density, that expresses the attenuation, due to diffusion, of the wave inside the medium.

When multiple scattering takes place, for instance when the density of scatterers is high (above 20%) and when their scattering power is important, the analytical expression of the effective dielectric constant is not accurate enough. This inaccuracy is observed if we compare the values of the coherently reflected and transmitted intensity of a slab filled of scatterers with that of a homogeneous film that has the same thickness and effective permittivity.[23] In this case, a numerical optimization of the effective permittivity is performed by studying the coherent transmission and reflection of the inhomogeneous slab for various thicknesses. This technique permits us to account for the diffusion losses that reduce the transmitted amplitude and is not restricted by the scattering amplitude or the density of the rods. Note, however, that the behavior of the mean field inside an inhomogeneous slab does not always follow that of the field inside an effective isotropic homogeneous film. Varying the angle of incidence may change the value of the effective permittivity. Yet in our examples concerning two-dimensional systems illuminated under s polarization with small scatterers, this approximation is usually valid. We used this numerical evaluation when the density of scatterers did not allow a good calculation of the diffusion losses.

We now come back to the empirical rule of the splitting of the scattering of rough inhomogeneous media into surface and volume contributions from a numerical point of view. The volume contribution is given by the *incoherent* intensity scattered by the particles placed in the binder beneath a flat surface. Note that by construction of the effective refractive index, the coherent intensity of the flat inhomogeneous medium is, in principle, equal to the specular peak given by the flat homogenized medium. The surface contribution is given by the total (coherent and incoherent) intensity scattered by the rough homogeneous effective surface. We have adopted this rule in all the following numerical experiments. It has enabled us to predict with accuracy the diffuse intensities and the specular reflected beam in many configurations of rough inhomogeneous media.

3. NUMERICAL STUDY

In this section we present several numerical experiments of scattering from rough inhomogeneous media to illus-

trate the splitting rule. These examples do not provide an exhaustive study of the validity of this interpretation. Indeed, the large number of parameters, rms height, correlation length, density of particles, scattering amplitude, and penetration depth (or permittivity contrast or losses) makes it a difficult task. They show, however, that the analysis of scattering from rough inhomogeneous media in terms of surface and volume contributions is reasonable well beyond the usual domain of validity of perturbation theories (i.e., small rms height, small scattering amplitude) and can also explain subtle scattering phenomena such as the shift of the Brewster angle. The numerical results presented in the following are obtained by averaging the scattering patterns over several hundred samples, each illuminated by a Gaussian beam with $w = 3\lambda$ or 4λ.

A. Beyond the Perturbative Domain

In this paragraph the light is *s* polarized and the particles are perfectly conducting cylinders with diameter 0.07 λ. Hence their scattering amplitude is important, so a perturbative treatment based on Born approximation is not possible. The rms height is moderate, 0.2–0.3 λ, but is also beyond height perturbative models. We study various densities of scatterers. Basically, we observe three configurations: (1) the volume scattering dominates, (2) the surface scattering dominates, or (3) they have roughly the same importance. In Fig. 3 the density of scatterers is $d = 0.03$, and the roughness parameters are $\sigma = 0.3\lambda$ and $l = \lambda$. With such a small density the scattering losses are very small, and the wave penetration depth is important if the binder is not lossy. For numerical reasons we have thus taken a binder with permittivity $\epsilon_b = 3 + i0.4$. Losses allow us to avoid very-long-range interactions and thus to limit the size of the system in both depth and width. The effective permittivity is calculated with the analytical model, Eq. (17), $\epsilon_{\text{eff}} = 3 + i0.6$. In this case the volume and surface contributions are of the same order, and their sum describes accurately the scattering of the rough inhomogeneous medium. Note that diminishing the binder losses increases the volume contribution. In Fig. 4 the permittivity of the binder is real and equal to $\epsilon_b = 2$. The density of scatterers is increased from 0.05 to 0.2. In Fig. 4(a), $d = 0.05$, the volume contribution dominates in such a way that the scattering from the flat inhomogeneous medium does not

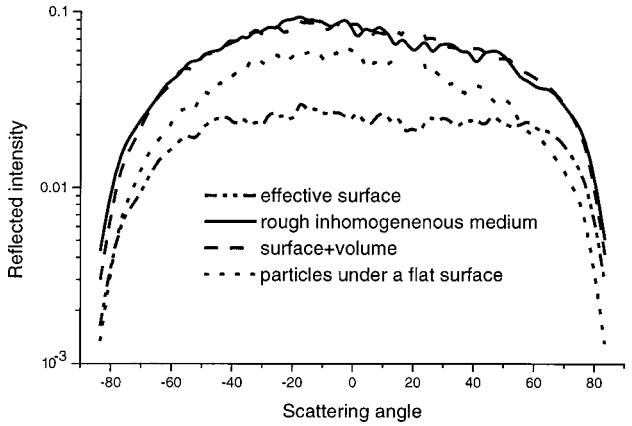

Fig. 3. Rough inhomogeneous medium illuminated under 20° of incidence; *s* polarization, $w = 3\lambda$. Binder, $\epsilon_b = 3 + i0.4$ $\sigma = 0.3\lambda$, $l = \lambda$. The cylindrical scatterers are perfectly conducting: $a = 0.035\lambda$, $d = 0.03\lambda$; the effective permittivity is calculated with Eq. (17) $\epsilon_{\text{eff}} = 3 + i0.6$.

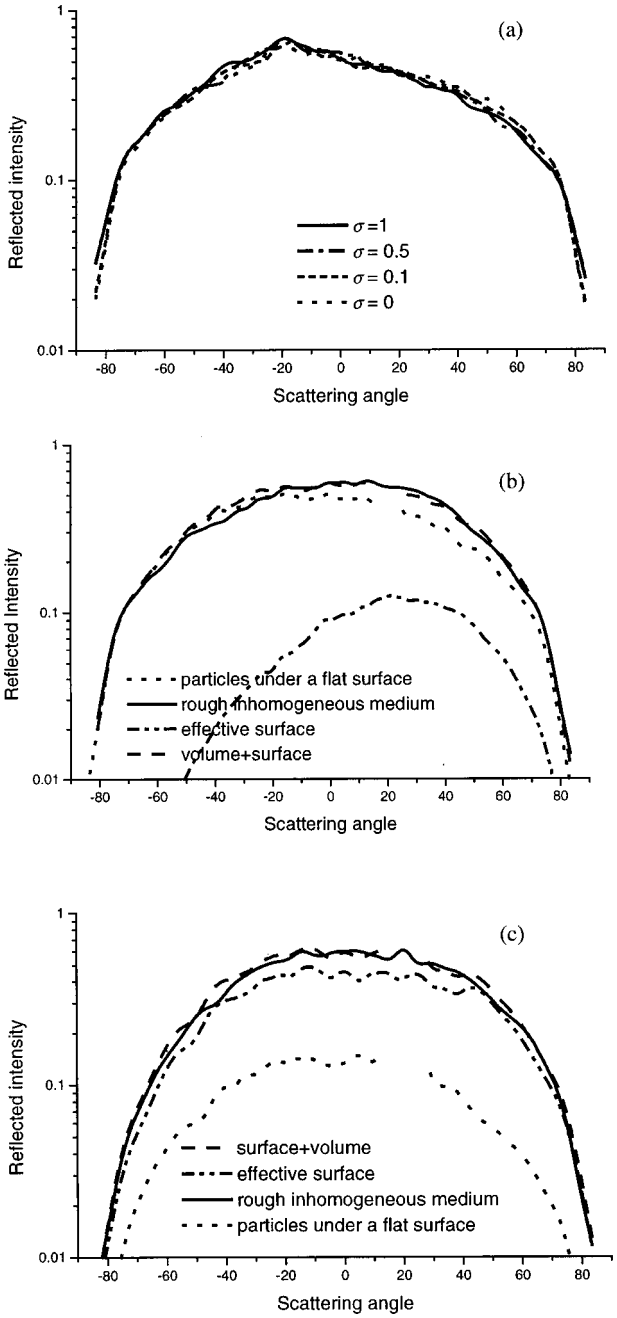

Fig. 4. Various geometries illuminated under 20° incidence; *s* polarization, $w = 4\lambda$. Binder, $\epsilon_b = 2$. The cylindrical scatterers are perfectly conducting $a = 0.035\lambda$. (a) $d = 0.05$, $l = \lambda$, various rms heights. The volume contribution dominates in such a way that changing the roughness does not affect the scattering pattern. (b) $d = 0.1$, $\sigma = 0.2\lambda$, $l = \lambda$. The effective surface contribution is increased and the penetration depth of the wave inside the volume is limited by the diffusion losses. The effective permittivity calculated with Eq. (17) is $\epsilon_{\text{eff}} = 0.67 + i1.95$. (c) $d = 0.2$, $\sigma = 0.2\lambda$, $l = 0.5\lambda$. The diffusion losses are important, the penetration depth is small, and the effective surface contribution dominates. The effective permittivity is obtained numerically by studying the coherent reflected energy of the inhomogeneous medium with a flat interface $\epsilon_{\text{eff}} = -7 + i3$.

present any specularly reflected beam. Following the splitting rule, this amounts to saying that the surface contribution is negligible. Indeed, the effective dielectric constant $\epsilon_{\text{eff}} = 1.34 + i0.9$ of the rough effective surface yields a scattering contribution that is 20 times smaller than the volume contribution. Hence, whatever the roughness, the scattering diagram remains the same. In Fig. 4(b) the volume density is 0.1. The effective permittivity given by Eq. (17) is $\epsilon_{\text{eff}} = 0.67 + i1.95$. The penetration depth of the wave inside the medium is thus reduced by the scattering losses. As a consequence, the volume contribution decreases, while it remains greater than the surface contribution. In Fig. 4(c) the density of scatterers is 0.2. In this case, the effective dielectric constant is evaluated numerically from the value of the coherent field reflected by the particles under a flat interface, $\epsilon_{\text{eff}} = -7 + i3$. The penetration depth is much smaller than λ, and the surface contribution dominates. Note that the effective surface behaves like a metallic medium even for small densities of scatterers. In all the previous examples, the splitting rule is accurate. Numerical experiments not shown here, with other angles of incidence, other correlation lengths, and other rms heights (the latter remaining in the moderate roughness range $<0.5\ \lambda$) have been performed with the same result. In contrast, we have encountered some difficulties when the roughness is increased. In Fig. 5 we study the splitting rule for an inhomogeneous medium with binder permittivity $\epsilon_b = 5 + i0.1$, scatterer density $d = 0.05$, correlation length λ, and two rms heights, $\sigma = 0.3\lambda$ and 0.7λ. The effective dielectric constant given by Eq. (17) is $\epsilon_{\text{eff}} = 4.4 + i1.3$. It is clear that the sum of the surface and volume contributions represents accurately the scattering from the inhomogeneous medium when $\sigma = 0.3\lambda$, whereas it underestimates that of the inhomogeneous medium when $\sigma = 0.7\lambda$. A possible reason for this discrepancy is that when the roughness is increased, the thickness of the perturbed region, contained between the highest and lowest incursions of the surface, is of the same order as the penetration depth of the wave. Hence the contribution to volume scattering of the particles that are present in this particular domain becomes important. In our opinion, estimating the volume contribution with the scattering pattern of particles under a flat interface is no longer accurate. Indeed, for the same finite spot, more particles are strongly illuminated under the rough surface than under the plane, as a consequence of the true length of the rough boundary. Thus, as it stands, the volume scattering is certainly underestimated.

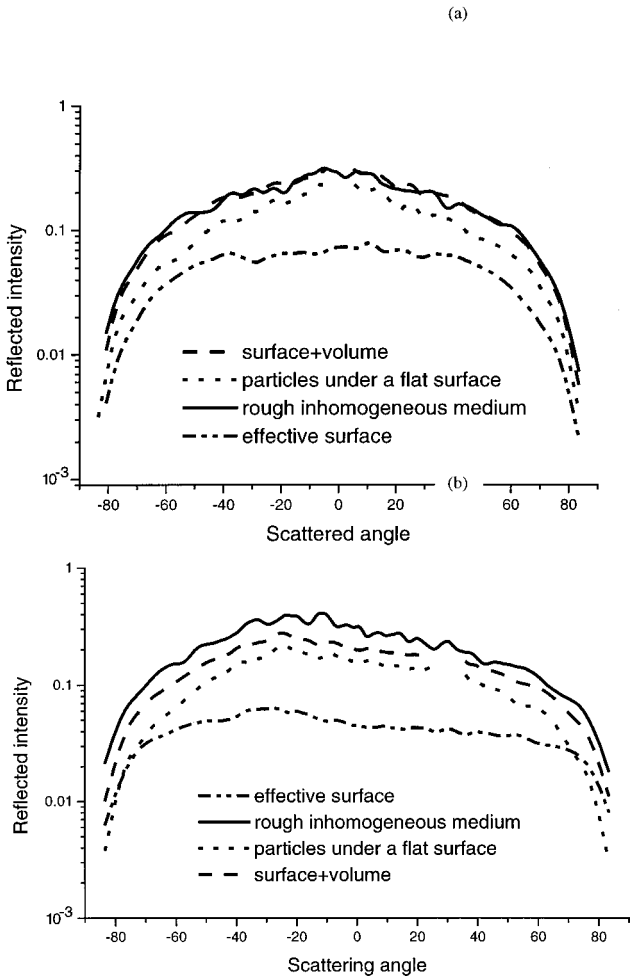

Fig. 5. Various geometries illuminated under *s* polarization; $w = 4\lambda$. Binder, $\epsilon_b = 5 + i0.1$; perfectly conducting scatterers: $d = 0.05$, $a = 0.035\lambda$. Effective permittivity calculated with Eq. (17) is $\epsilon_{\text{eff}} = 4.4 + i1.3$. (a) $\sigma = 0.3\lambda$, $l = \lambda$, normal incidence; the splitting rule works. (b) $\sigma = 0.7\lambda$, $l = \lambda$, 30° of incidence; the splitting rule is not accurate.

B. Brewster Incidence

In this subsection a rough surface is illuminated under *p* polarization around Brewster's angle. In these conditions, the volume-scattering contribution is enhanced, and it is also interesting to study the shift of Brewster's angle. The reflectivity of a flat surface illuminated under Brewster's angle is null. It has been shown with a second-order small-perturbation method[24] that when the surface is slightly rough, the specularly reflected (coherent) intensity presents a minimum for an incident angle close to but smaller than the Brewster angle. In the following, we show that volume scattering modifies this shift in accordance with basic homogenization rules.

The rods are circular in shape, with radius $a = 0.05\lambda$, and their volume fraction is $d = 3\%$. They are embedded in a lossy medium, with complex permittivity $\epsilon_b = 2 + i0.1$. In the presence of losses, the reflection coefficient for a flat interface no longer vanishes, but here a deep minimum still exists at Brewster's angle, approximately 54°76. Two kinds of rods are considered: one with lower permittivity than the embedding medium ($\epsilon_{\text{sc}} = 1$), Figs. 6(a) and 6(b), and one with higher permittivity ($\epsilon_{\text{sc}} = 5$), Figs. 6(c) and 6(d). With such a low density, volume scattering is mainly single scattering. The surface roughness parameters are $\sigma = 0.05\lambda$, and the correlation length is $l = 0.5\lambda$. The random medium is illuminated by a Gaussian beam with $w = 3\lambda$ and $\theta^{\text{inc}} = 55°$. Using such a relatively narrow beam permits us to give more obvious evidence of Brewster's phenomenon. Indeed, it can be seen in Figs. 6(a) and 6(b) that the specularly reflected beam extends roughly from 45° to 80° and exhibits a deep minimum around Brewster's angle.

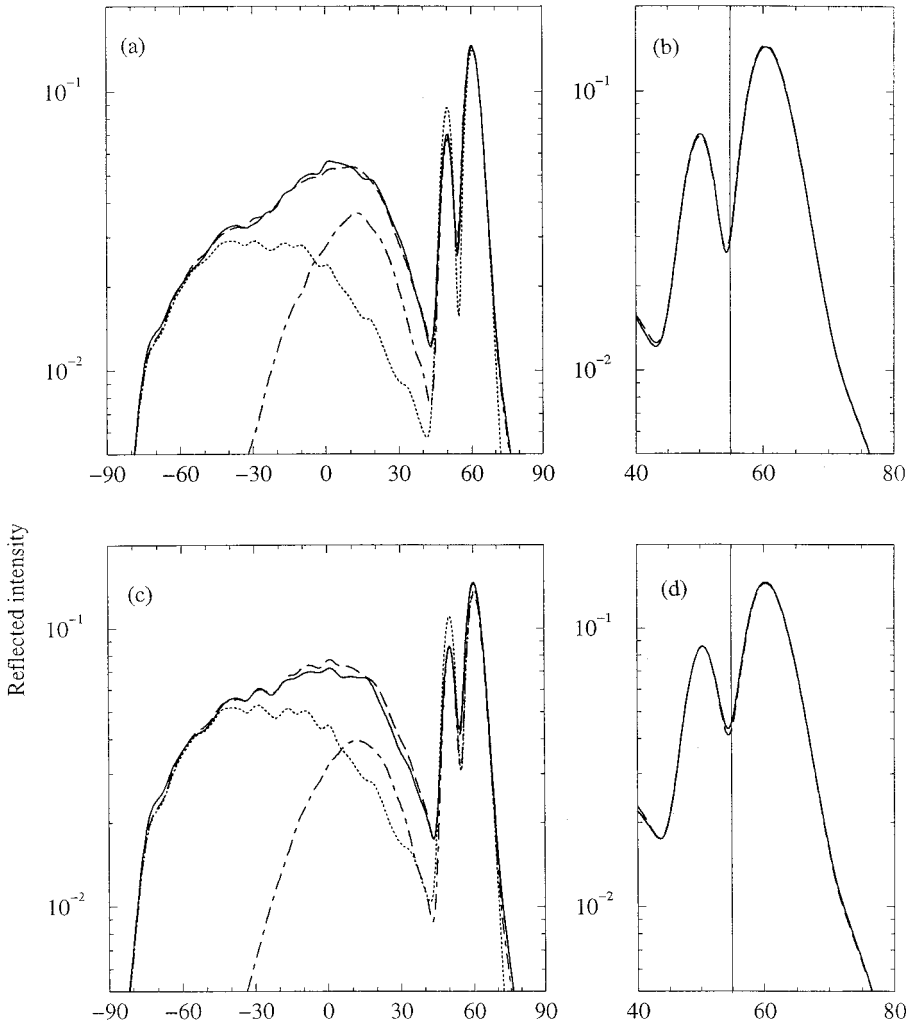

Fig. 6. Scattered patterns of various geometries illuminated under 55° of incidence; p polarization, $w = 3\lambda$. A zoom about the Brewster angle of the binder (54°76) is given in (b) and (d). Binder, $\epsilon_b = 2 + i0.1$; $\sigma = 0.05\lambda$, $l = 0.5\lambda$. Scatterers, $d = 0.03$, $a = 0.05$. (a) and (b), $\epsilon_{sc} = 1$; (c) and (d), $\epsilon_{sc} = 5$. Solid curves, reflected intensity of the rough inhomogeneous medium; dotted curves, particles under a flat surface (volume); dashed–dotted curves, effective surface; dashed curves, scattered intensity of the volume plus that of the effective surface, minus the reflection from a plane with the effective permittivity. (b) and (d), solely the dash and solid curves are plotted.

The shift of Brewster's angle is estimated from the location of the minimum of the scattered intensity. As usual, the four plotted curves represent the contributions of the effective surface: of the rods under a flat interface and of the sum of these two (after one specular reflection is removed) to be compared with the scattering pattern of the rough inhomogeneous medium. The latter two plots are amazingly close to each other both for permittivity contrast and in and out of the specular region. This result shows that the splitting rule can also express very fine effects. Let us focus now on the minima of the various patterns around Brewster's angle. If $\epsilon_{sc} = 5$, the effective permittivity, given by Eq. (17) or Bruggeman formula Eq. (14), is $\epsilon_{eff} \approx 2.05 + i0.1$. Therefore, if the effective permittivity is increased compared with that of the binder, the rods create a displacement of the minimum toward larger angles. In contrast, for air bubbles ($\epsilon_{sc} = 1$), since the effective permittivity is smaller than that of the binder, both surface and volume effects shift the minimum toward lower angles. This explains why the minimum in Fig. 6(d) occurs at larger angles than in Fig. 6(b).

Another example of the well-foundedness of the splitting rule and of the importance of a good evaluation of the effective permittivity is presented in Section 4.

4. REDUCTION OF SURFACE SCATTERING

It has been demonstrated that coatings deposited on rough homogeneous surfaces can lead to a scattering-reduction effect. This effect, which has been studied both theoretically and experimentally, was first observed with smooth surfaces[25] and afterward in the resonance domain.[26,27] It has been found that the strongest scattering-reduction effect is always obtained with classical antireflection layers. In this section we extend this study to the case of rough inhomogeneous surfaces.

For a given rough homogeneous surface the performance of a scattering-reduction coating depends strongly on its optogeometrical parameters (e.g., thickness and permittivity). Designing the coating for obtaining the lowest scattering level requires knowledge of the permit-

tivity of the bare surface. In all the cases the profile of the bare surface is assumed to be perfectly replicated by the coating. The method used for determining thickness h and permittivity ϵ of the antireflection layer is the same as the one used for optical thin-film applications. h and ϵ are chosen so that destructive interference between the waves reflected at each interface (air/layer and layer/substrate) occur. Among the solutions obtained, the one with a real value of ϵ is retained in order to eliminate spurious effects on the scattering level that are due to absorption in the coating. We denote by ϵ_s the permittivity of the substrate. In this case,

$$h = \frac{\lambda}{2\pi\sqrt{\epsilon}} \arctan\left[\frac{\sqrt{\epsilon}(n_s - 1)}{k_s}\right], \tag{18a}$$

with

$$\epsilon = \frac{k_s^2}{n_s - 1} + n_s, \tag{18b}$$

where

$$n_s + ik_s = \sqrt{\epsilon_s}.$$

Since so far the study of scattering-reduction coatings has been carried out only for homogeneous dielectric surfaces, the question that arises is whether a scattering-reduction effect can be obtained in the case of rough inhomogeneous media and how the optogeometrical parameters of the coating can be determined.

We have tested the behavior of the rough inhomogeneous medium studied in Fig. 2 (Section 2), covered by an antireflection layer optimized for the binder. One can see in Fig. 7(a) that the amount of scattered energy is lower than for the bare inhomogeneous medium. The results of Sections 2 and 3 suggest that a better performance can be obtained by taking into account the permittivity ϵ_{eff} of the effective medium. This is confirmed by the results of Fig. 7(a). The antireflection coating optimized for ϵ_{eff} strongly reduces the total amount of scattered energy and gives a better scattering-reduction effect than the antireflection coating optimized for ϵ_b. However, as the transmitted energy is stronger, it leads to an enhancement of volume scattering. This effect, which is clearly visible in Fig. 7(a), is stronger at high scattering angles because volume scattering is predominant at high spatial frequencies. The result is that at high scattering angles, the scattered energy is stronger for the coated medium than for the bare one. Figure 7(b) shows that the angular behavior of the scattering pattern of the coated rough inhomogeneous medium resembles that of the coated flat inhomogeneous medium. The observed difference in the vicinity of the specular beam stems from the residual scattering contribution of the effective surface that has not been totally eliminated by the coating.

These results generalize those obtained for homogeneous surfaces. Surface scattering can be nearly eliminated by depositing an appropriate coating, even in the case of inhomogeneous media. For better results, the optogeometrical parameters of the coating should account for the value of the effective permittivity of the random medium. In this case an enhancement of volume scattering is obtained.

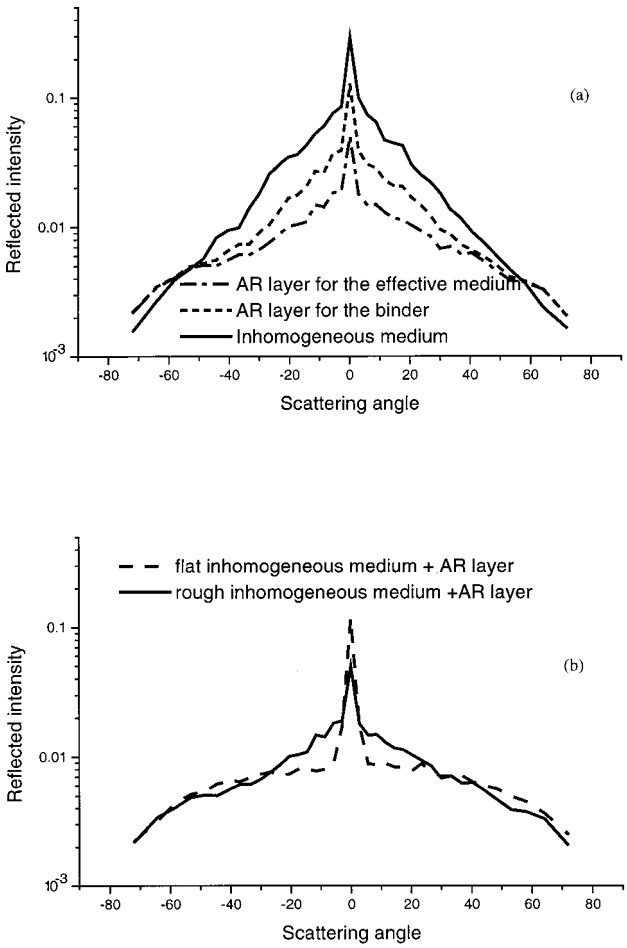

Fig. 7. Scattering-reduction effect obtained with two different coatings deposited on a rough inhomogeneous medium. Parameters of the medium are the same as in Fig. 2. The value of the effective permittivity ϵ_{eff} was determined numerically by studying the specularly reflected and transmitted field of slabs of the random medium with different thicknesses $\epsilon_{\text{eff}} = 2.35 + i0.65$. When the antireflection (AR) layer is optimized for the binder, its permittivity is $\epsilon = \epsilon_b{}^{0.5} = 1.41$ and thickness $h = \lambda/4\epsilon_b{}^{0.5} = 0.21\lambda$. When the layer is optimized for the effective medium Eqs. (18), $\epsilon = 1.627$ and $h = 0.159\lambda$.

5. CONCLUSION

We have shown that the scattering pattern of rough inhomogeneous media can be explained in terms of surface- and volume-scattering contributions. The volume contribution is obtained by evaluating the incoherent scattering from particles placed in the binder under a flat surface. The surface contribution is given by the scattering of a rough homogeneous surface whose permittivity accounts for the presence of the particles in the binder. This permittivity is obtained either analytically with effective-medium theories or numerically by studying the coherently reflected and transmitted beams of a slab of the inhomogeneous medium. The splitting rule works well beyond the usual validity domains of perturbation theo-

ries, even if multiple scattering occurs in the volume or on the surface. The incoherent scattering is well represented by the sum of the two contributions, and the specular peak is also retrieved. With this rule, we can explain the shift of the Brewster angle for inhomogeneous rough media. By depositing on the inhomogeneous medium a coating that is optimized for the effective rough homogeneous surface, we are able to diminish the surface contribution and thus enhance the volume scattering. The splitting process permits us to interpret scattering diagrams and to simplify the numerical calculations by treating the volume and surface problems separately. Yet some improvements should be evident when the roughness is of the same order as the penetration depth of the wave inside the random medium. Indeed, if the contribution of the particles just below the surface is important, the volume scattering cannot be described simply by that of the flat binder full of particles.

Corresponding author Anne Sentenac can be reached by e-mail at anne.sentenac@fresnel.fr.

References

1. L. Tsang, G. Kong, and R. Shin, *Theory of Microwave Remote Sensing* (Wiley Interscience, New York, 1985).
2. K. Fung, *Microwave Scattering and Emission Models and Their Applications* (Artech House, Boston, Mass., 1994).
3. C. Lam and A. Ishimaru, "Mueller matrix representation for a slab of random medium with discrete particles and random rough surfaces with moderate surface roughness," Math. Gen. **260**, 111–125 (1993).
4. J. M. Elson, "Theory of light scattering from a rough surface with an inhomogeneous dielectric permittivity," Phys. Rev. B **30**, 5460–5480 (1984).
5. K. Sarabandi, Y. Oh, and F. Ulaby, "A numerical simulation of scattering from one-dimensional inhomogeneous dielectric rough surfaces," IEEE Trans. Geosci. Remote Sens. **34**, 425–432 (1996).
6. S. Mudaliar, "Electromagnetic wave scattering from a random medium layer with random interface," Waves Random Media **4**, 167–176 (1994).
7. S. Dietrich and A. Haase, "Scattering of x-rays and neutrons at interfaces," Phys. Rep. **260**, 1–138 (1995).
8. S. K. Sinha and E. B. Sirota, and S. Garoff, "X-ray and neutron scattering from rough surfaces," Phys. Rev. B **38**, 2297–2311 (1988).
9. A. Sentenac and J.-J. Greffet, "Mean-field theory of light scattering by one-dimensional rough surfaces," J. Opt. Soc. Am. A **15**, 528–532 (1998).
10. O. Calvo-Perez, A. Sentenac, and J.-J. Greffet, "Light scattering by a two-dimensional, rough penetrable medium: a mean-field theory," Radio Sci. **34**, 311–335 (1999).
11. A. Madrazo and M. Nieto-Vesperinas, "Scattering of light and other electromagnetic waves from a body buried beneath a highly rough random surface," J. Opt. Soc. Am. A **14**, 1859–1866 (1997).
12. G. Zhang, L. Tsang, and K. Pak, "Angular correlation function and scattering coefficient of electromagnetic waves scattered by a buried object under a two-dimensional surface," J. Opt. Soc. Am. A **15**, 2995–3002 (1998).
13. K. Pak, L. Tsang, L. Li, and C. Chan, "Combined random rough surface and volume scattering based on Monte-Carlo solutions of Maxwell's equation," Radio Sci. **28**, 331–338 (1993).
14. G. Pelosi and R. Coccioli, "A finite element approach for scattering from inhomogeneous media with a rough interface," Waves Random Media **7**, 119–127 (1997).
15. G. Zhang, L. Tsang, and Y. Kuga, "Angular correlation function of wave scattering by a buried object embedded in random discrete scatterers under a rough surface," Microwave Opt. Technol. Lett. **14**, 144–151 (1997).
16. H. Giovannini, M. Saillard, and A. Sentenac, "Numerical study of scattering from rough inhomogeneous films," J. Opt. Soc. Am. A **15**, 1182–1191 (1998).
17. O. Calvo, "Diffusion des ondes électromagnétiques par un film rugueux hétérogène," Ph.D. thesis (Ecole Centrale Paris, 1999).
18. L. Li, "Formulation and comparison of two recursive matrix algorithms for modeling layered diffraction gratings," J. Opt. Soc. Am. A **13**, 1024–1035 (1996).
19. L. Li, "Use of Fourier series in the analysis of discontinuous periodic structures," J. Opt. Soc. Am. A **13**, 1870–1876 (1996).
20. C. Bohren and D. Huffman, *Absorption and Scattering by Small Particles* (Wiley, New York, 1983).
21. U. Frish, "Wave propagation in random media," in *Probabilistic Methods in Applied Mathematics*, A. T. Bharucha-Reid, ed. (Academic, New York, 1968), pp. 75–197.
22. J. B. Keller, "Stochastic equations and wave propagation in random media," Proc. Symp. Appl. Math. **16**, 145–170 (1964).
23. A. Ishimaru and Y. Kuga, "Attenuation constant of a coherent field in a dense distribution of particles," J. Opt. Soc. Am. **72**, 1317–1320 (1982).
24. M. Saillard, "A characterization tool for dielectric random rough surface: Brewster phenomenon," Waves Random Media **2**, 67–79 (1992).
25. C. Amra, G. Albrand, and P. Roche, "Theory and application of antiscattering single layers: antiscattering antireflection coatings," Appl. Opt. **25**, 2695–2702 (1986).
26. H. Giovannini and C. Amra, "Scattering-reduction effect with overcoated rough surfaces: theory and experiment," Appl. Opt. **36**, 5574–5579 (1997).
27. H. Giovannini and C. Amra, "Dielectric thin films for maximized absorption with standard quality black surfaces," Appl. Opt. **37**, 103–105 (1998).